Rate/state frictional nucleation and dynamic rupture on low-stress faults with thermal weakening effects

Stuart V. Schmitt, Andrew M. Bradley, Eric M. Dunham, *and* Paul Segall
Department of Geophysics, Stanford University

INTRODUCTION

It is believed that faults sustain large shear stresses during the nucleation phase, but slip at much lower stresses during earthquakes. Nucleation is typically characterized by rate- and state-dependent friction, in which slip accelerates after shear stress τ grows to about 0.6 to 0.9 times the effective normal stress σ. During earthquakes, dynamic weakening mechanisms such as shear heating-induced thermal pressurization of pore fluid and flash heating of asperity contacts allow for slip to occur at much lower values of τ. Since 0.6σ is ~100 MPa at seismogenic depths with hydrostatic pore pressure, earthquakes likely nucleate in regions of elevated τ/σ and propagate outward into regions of low τ/σ.

Noda, Dunham, & Rice [JGR, 2009] investigated slip at low τ/σ with numerical simulations in which they included both flash weakening and thermal pressurization. The rupture mode (crack-like or pulse-like) for a strongly rate-weakening fault depends on the pre-existing stress state on the fault, with pulse-like rupture occurring only on faults with low background shear stress. *Noda & others* artificially initiated ruptures with a sudden perturbation in τ on a weakly stressed fault. Flash heating quickly dominated the fault strength, with thermal pressurization contributing a modest amount of additional weakening. Thermal pressurization and the nucleation zone dimension also affected the rupture mode.

Recent work has shown that thermal pressurization may, however, become the dominant weakening mechanism during quasi-static nucleation, well before the onset of seismic radiation [*Schmitt, Segall, & Matsuzawa*, JGR, 2011]. Thermal pressurization is effectively a slip weakening mechanism that feeds back into itself. For crack-like nucleation, which aging-law friction exhibits, thermal pressurization rapidly dominates in the center of the slip zone. This effect leads to dramatic along-strike localization of the nucleation zone. The pulse-like nature of slip-law nucleation lessens the feedback process, yet thermal pressurization is significant late in nucleation for a wide range of fault parameters.

We present more physically-motivated simulations of nucleation and early rupture that model fault weakening mechanisms through nucleation and into the dynamic slip phase, though we neglect flash weakening in the work shown here. The initial τ/σ heterogeneities remain idealized, but we now consider two types. The first type is a region of elevated τ with uniform σ, while the other type has uniform τ with a low-strength region of diminished σ.

GOVERNING EQUATIONS

Rate- and state-dependent friction:

$$\tau = \left[\mu_0 + a\ln\frac{v}{v_0} + b\ln\frac{\theta v_0}{d_c}\right](\sigma - p)\,. \qquad (1)$$

State evolution laws:

$$\frac{d\theta}{dt} = 1 - \frac{v\theta}{d_c}\ \text{(aging law)} \quad \text{and} \quad \frac{d\theta}{dt} = -\frac{v\theta}{d_c}\ln\frac{v\theta}{d_c}\ \text{(slip law).} \qquad (2)$$

Equation of motion with constant, uniform, shear loading:

$$\tau = \tau_0(x) + \dot{\tau}\,t - \frac{G}{2v_s}v + \phi(x,t)\,. \qquad (3)$$

Elastic stress interaction:

$$\phi(x,t) = \int_0^t \int_{-\infty}^{\infty} K(x-x', t-t')\,u(x',t')\,dx'\,dt'\,. \qquad (4)$$

Thermal diffusion and shear heating on a finite-width fault:

$$\frac{\partial T}{\partial t} = c_{\text{th}}\frac{\partial^2 T}{\partial y^2} + \frac{\omega(y,t)}{\rho c_v} \quad \text{and} \quad \omega(y,t) = \frac{\sqrt{2}\tau v}{\sqrt{\pi}h}\exp\left(-\frac{2y^2}{h^2}\right). \qquad (5)$$

Pore pressure generation and transport:

$$\frac{\partial p}{\partial t} = c_{\text{hyd}}\frac{\partial^2 p}{\partial y^2} + \Lambda\frac{\partial T}{\partial t} \quad \text{with} \quad \Lambda = \frac{\lambda_f - \lambda_\phi}{\beta_f + \beta_\phi}\,. \qquad (6)$$

Minimum half-width for a slip zone capable of becoming an earthquake:

$$L_{\text{min}} = \frac{Gd_c}{2(b-a)(\sigma - p)}\,. \qquad (7)$$

Half-width of aging law nucleation zone late in nucleation phase:

$$L_\infty = \frac{Gbd_c}{\pi(b-a)^2(\sigma - p)}\,. \qquad (8)$$

Fault parameters

G	shear modulus	10 GPa
v_s	s-wave velocity	3700 m/s
v_p	p-wave velocity	6409 m/s
$\dot{\tau}$	shear loading rate	0.01 Pa/s
$\sigma - p_0$	ambient eff. normal stress	126 MPa
μ_0	nominal friction	0.7
a	friction velocity effect	0.016
b	friction state effect	0.020
d_c	slip weakening distance	20 μm
h	shear zone thickness	100 μm
c_{th}	thermal diffusivity	0.7 mm²/s
c_{hyd}	hydraulic diffusivity	2.988 mm²/s
ρc_v	density × heat capacity	2.86 MPa/°C
Λ	thermal coupling param.	0.468 MPa/°C
λ_f	pore fluid expansivity	
λ_ψ	pore expansivity	
β_f	pore fluid compressibility	
β_ψ	pore compressibility	
w	width of heterogeneity	$2.5L_{\text{min}}$ & $2L_\infty$
L_{min}	minimum nuc. zone size	0.26 m (HS sim.)
L_∞	aging law nuc. zone size	8.4 m (LS sim.)
K	static or dynamic elastic kernel	
θ	frictional state	
v	slip speed	
u	slip	
T	temperature (change)	
p	pore pressure (change)	
σ	normal stress	
τ	shear stress	

MODEL & METHODS

We model the fault as a boundary of a 2D finite difference diffusion grid. The fault is initialized with a uniform low slip speed and an initial stress described in the next section. We impose a uniform shear stressing rate. The fault ends satisfy a periodic boundary condition.

For the nucleation phase, we use the quasi-static code *FDRA* [*Bradley & Segall*, AGU, 2010], which is capable of integrating the coupled diffusion system rapidly during times of little evolution. Shortly before seismic radiation becomes significant, we export values of slip, fault state, stress, temperature, and pore pressure to *MDSBI*, an elastodynamic code [*Noda & others*, 2009]. Apart from the stress interaction term, both codes solve the same governing equation. Both codes use the spectral boundary integral equation method for elasticity and feature adaptive substepping for diffusion during elasticity time steps.

TWO SIMPLE MODELS OF τ/σ HETEROGENEITY

Two simple stress models can satisfy a given $\tau/(\sigma - p)$ profile. In one, there is a concentration of shear stress, while effective normal stress is uniform. We call this the **high stress model**. In the other, shear stress is uniformly low, while there is a region of diminished effective normal stress. We call this the **low strength model**.

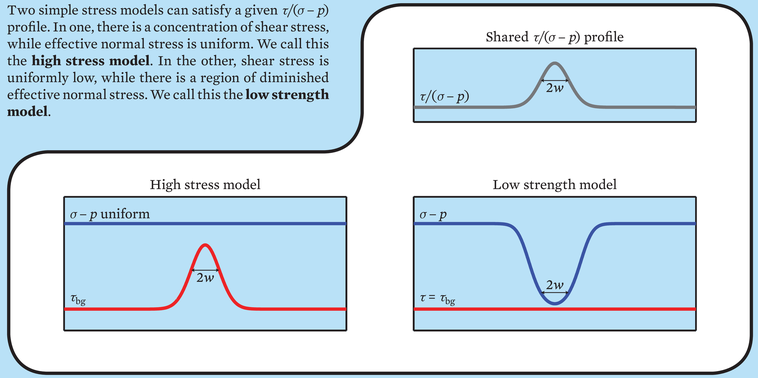

SAMPLE HIGH STRESS SIMULATION

The results below are space-time plots from a high-stress simulation that uses slip-law friction. The time axis has two scales; the rate/state nucleation phase occurs over years leading up to $t = 0$, and is followed by the initiation of seismic rupture during a few tenths of a millisecond. The small-scale "ringing" features in the velocity plot are a consequence of coarse discretization along the fault, which causes the spectral method to be unable to resolve large stress drops. The simulation terminated when there was a total loss of numerical accuracy. The coarse discretization was chosen for the purpose of prototyping future, larger models.

In the last few seconds of the nucleation phase, a slip pulse grows in the $+x$ direction. During dynamic rupture, slip propagates at subshear speed into the low-stress background region (UPPER LEFT). In the other direction, a high stress concentration remains. Rupture attains supershear speed as it propagates across the highly-stressed region.

Thermal pressurization is substantial in this model. Significant heating (LOWER RIGHT) causes thermal pressurization to result in a total stress drop in the slip zone (UPPER RIGHT).

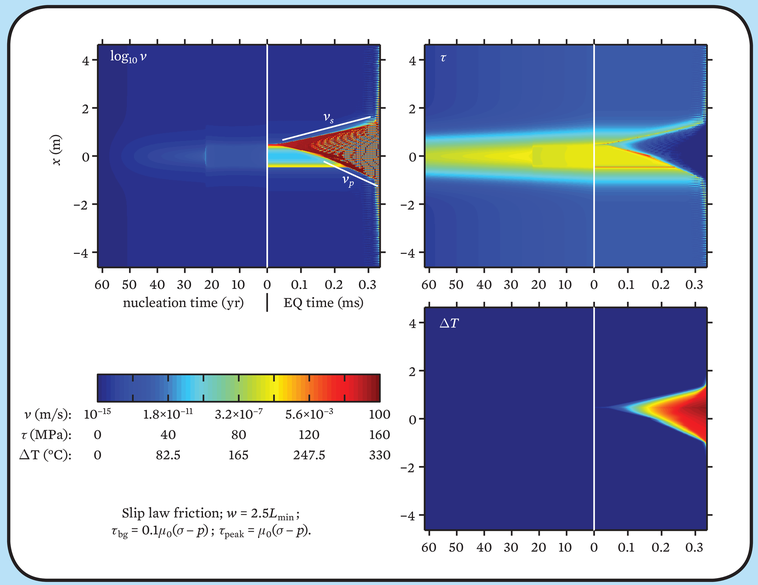

SAMPLE LOW STRENGTH SIMULATION

The results below are from a low-strength simulation using aging-law friction. The spatial scale is much larger than for the high-stress model because $L_\infty \propto \sigma^{-1}$ (and further, $L_\infty > L_{\text{min}}$). Like the high-stress simulation, this simulation suffers from inadequate spatial resolution, but in this case the stress drops are sufficiently small that the simulation is able to proceed until the rupture terminates.

Under the aging law, thermal pressurization leads to localization of slip in the middle of the nucleation zone as slip accelerates above ~1 mm/s. Dynamic slip initiates there and rapidly traverses the nucleation zone. Once outside the nucleation zone, propagation continues at subshear speeds until the rupture terminates (UPPER LEFT). The stress drop is nearly complete inside the slip zone (UPPER RIGHT). Heat generation is weak in the low $(\sigma - p)$ region, though large but transitory "hot spots" occur as slip enters the high background $(\sigma - p)$ region (LOWER RIGHT).

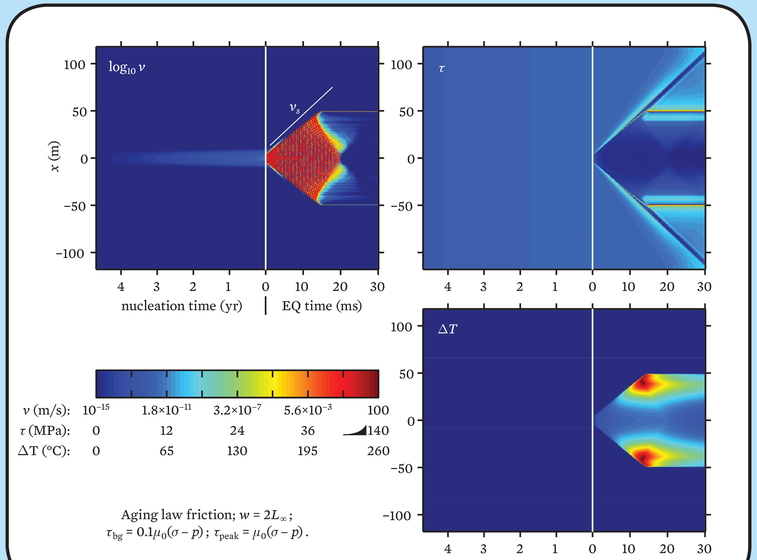

OBSERVATIONS

Because slip occurs at high stress, much more heat is generated in high-stress ruptures than low-strength ruptures. Thermal pressurization is therefore much stronger. A huge stress drop inside the nucleation region leads to a very energetic initial phase of seismic slip. Since $L_{\text{min}} \propto (\sigma - p)^{-1}$, the size of a high-stress nucleation zone is much smaller than a low-strength nucleation zone.

Thermal pressurization is weak in low-strength ruptures. Interestingly, however, the speed at which thermal pressurization dominates rate/state frictional weakening is independent of $(\sigma - p)$ [see *Schmitt & others*, 2011]. Significant heat and pore fluid pressurization occurs as slip propagates into the high $(\sigma - p)$ region. These temperature and pore pressure anomalies rapidly diffuse away.

For a given uniform shear loading rate, wider heterogeneities allow for instability to occur at lower background shear stress τ_{bg}. For Gaussian heterogeneities, $w > 2L_{\text{min}}$ is required for slip law friction, while $w > 2L_\infty$ is required for aging law friction.

Because of its pulse-like nature, dynamic slip under slip-law rate/state friction initiates at the edge of the nucleation zone. Aging law nucleation, on the other hand, tends to accelerate to dynamic slip speeds in the middle of the nucleation zone.

CONCLUSION

The simulations shown here are greatly simplified. Much greater spatial resolution is necessary to model dynamic slip correctly. We have also neglected important physics—in particular, flash weakening of asperity contacts is not included, but is likely a significant dynamic weakening mechanism at high slip speeds. Our codes are already capable of addressing those issues.

Predictions of these models may be on the cusp of observability for small, natural earthquakes if sensors are located close to the seismic source (for example, in mines or boreholes). The two ruptures shown here have potentially observable differences in their average stress drop, moment rate history, and residual thermal anomaly.